Hydrological connectivity of hillslopes and streams: Characteristic time scales and nonlinearities

Kevin J. McGuire[1] and Jeffrey J. McDonnell[2,3]

[1] Subsurface flow from hillslopes is widely recognized as an important contributor to streamflow generation; however, processes that control how and when hillslopes connect to streams remain unclear. We investigated stream and hillslope runoff dynamics through a wet-up period in watershed 10 of the H. J. Andrews Experimental Forest in the western Cascades of Oregon where the riparian zone has been removed by debris flows. We examined the controls on hillslope-stream connectivity on the basis of observations of hydrometric, stable isotope, and applied tracer responses and computed transit times for multiple runoff components for a series of storms during the wet-up phase of the 2002–2003 winter rainy season. Hillslope discharge was distinctly threshold-like with a near linear response and average quick flow ratio of 0.58 when antecedent rainfall was greater than 20 mm. Hillslope and stream stormflow varied temporally and showed strong hysteretic relationships. Event water mean transit times (8–34 h) and rapid breakthrough from applied hillslope tracer additions demonstrated that subsurface contributing areas extend far upslope during events. Despite rapid hillslope transport processes during events, soil water and runoff mean transit times during nonstorm conditions were greater than the time scale of storm events. Soil water mean transit times ranged between 10 and 25 days. Hillslope seepage and catchment base flow mean transit times were between 1 and 2 years. We describe a conceptual model that captures variable physical flow pathways, their synchronicity, threshold activation, hysteresis, and transit times through changing antecedent wetness conditions that illustrate the different stages of hillslope and stream connectivity.

1. Introduction

[2] Although it is generally acknowledged that subsurface flow dominates runoff in forested catchments, specific pathways, residence times and sources of water often remain unclear [*Bonell*, 1998; *Kirchner*, 2006; *Lischeid*, 2008]. In particular, the processes that hydrologically connect uplands with the stream network are still not well understood or quantified [*Bracken and Croke*, 2007; *Ali and Roy*, 2009; *Hopp and McDonnell*, 2009]. Hydrological connectivity between uplands (also known as the hillslopes) and the stream or riparian network has been defined in many ways, but perhaps it is most commonly used to describe when water tables develop between the hillslope and riparian zone [*Vidon and Hill*, 2004; *Ocampo et al.*, 2006] and result in a measurable runoff response [*Bracken and Croke*, 2007]. Recent studies have shown that the hillslope connection depends on catchment wetness, soil properties and surface and bedrock topography [*Freer et al.*, 1997; *Sidle et al.*, 2000; *Buttle et al.*, 2004; *Jencso et al.*, 2009; *Detty and McGuire*, 2010a] and in some cases, hillslopes only rarely connect to the stream environment [*Tromp-van Meerveld and McDonnell*, 2006a]. This hydrologic coupling between hillslopes and the riparian zone or stream network is prerequisite for the delivery of solutes downslope to the stream [*Hooper et al.*, 1998; *Stieglitz et al.*, 2003; *Burt and Pinay*, 2005] and represents an important emergent behavior at the landscape scale. Nevertheless, quantifying these connections at the catchment scale is difficult because hillslope contributions are often initiated only after exceeding a storage threshold [*Spence and Woo*, 2003; *Buttle et al.*, 2004; *Kim et al.*, 2004; *Tromp-van Meerveld and McDonnell*, 2006a, 2006b; *Detty and McGuire*, 2010b] or they are obscured by throughflow spatial variability and preferential flow [*Woods and Rowe*, 1996; *Hopp and McDonnell*, 2009]. Most problematic for understanding and quantifying the hillslope-stream connection is the presence of riparian zones that water from the hillslope must pass through prior to contributing to streamflow [*Robson et al.*, 1992; *McGlynn and McDonnell*, 2003]. Riparian zones both modulate and obscure hillslope signals. Devising new ways to detect, quantify and understand the linkages between processes in the uplands and the aquatic environment remains one of the most pressing chal-

---

[1] Virginia Water Resources Research Center and Department of Forest Resources and Environmental Conservation, Virginia Polytechnic Institute and State University, Blacksburg, Virginia, USA.

[2] Department of Forest Engineering, Resources and Management, Oregon State University, Corvallis, Oregon, USA.

[3] School of Geosciences, University of Aberdeen, Aberdeen, UK.

lenges in environmental hydrology [e.g., see *Ali and Roy*, 2009].

[3] Here we take advantage of a catchment with an unobstructed hillslope signal where the riparian zone has been largely removed from a history of debris flows. The catchment runoff response therefore expresses a relatively unmodified input of multiple hillslope segments with no riparian aquifer influence impeding hydrologic connectivity (i.e., when hillslopes contribute runoff). We further leverage the very clear seasonality of our site with distinct and extended wet and dry seasons that accentuate connectivity presence and absence. We focus on a well-studied planar sideslope (first reported on by *Harr* [1977]) during a wet-up period that begins with extremely dry soil conditions and progressively increases in wetness. We then quantify the hillslope contributing area that connects and delivers water and solute to the stream network.

[4] Hydrologic connectivity is often dynamic in that connections/disconnections occur seasonally and episodically during events. Even though a connection may occur between a hillslope and the stream or between two regions of the landscape, it does not necessarily suggest that water travels between those regions over the time scale of an event. Therefore in addition to characterizing connections between the hillslope and stream and potential runoff generation, it is necessary to quantify the transport time scale or transit times of water as it moves from the hillslope to the stream. Since runoff can be in the form of event water (i.e., runoff derived from the rainfall or snowmelt event itself) or preevent water (i.e., runoff derived from water stored in the catchment prior to the event), the transit times of these separate runoff components become important metrics of hydrologic connectivity. In this study, we base our observations and constrain our conceptualization of hillslope-stream connectivity on hydrometric, stable isotope, and applied tracer responses following recommendations by *Bonell* [1998] and *Burns* [2002] and compute transit time distributions for various runoff components. These data resources allow us to reject many possible behaviors to decipher and explore the physical controls on runoff generation and hillslope-stream connectivity on a well-studied hillslope. Consequently, we test the following null hypotheses: (1) the hillslope runoff is linearly related to the catchment runoff, (2) hillslopes are not capable of transporting solutes (tracer) to the stream from upslope areas over the time scale of a storm event, (3) event water contributions are similar for the hillslope and catchment, and (4) hillslope transit time increases downslope and is similar to the stream when it reaches the slope base.

[5] By testing these hypotheses we attempt to constrain a new conceptualization of hydrological connectivity of hillslopes and streams, aimed for the first time at characteristic time scales and nonlinearities.

2. Site Area and Methods

[6] The study was conducted in watershed 10 (WS10, 10.2 ha) at the H. J. Andrews Experimental Forest (HJA) in the west central Cascade Mountains of Oregon, USA (44.2°N, 122.25°W) (Figure 1). WS10 was the location of intensive forest ecological research as part of the U.S. International Biological Program's Coniferous Forest Biome project [*Sollins et al.*, 1980; *Gholz et al.*, 1984; *Triska et al.*, 1984]

and is currently part of the NSF Long-Term Ecological Research (LTER) program at the HJA. Elevations range from 473 m at the flume to 680 m at the catchment divide. Annual precipitation is 2220 mm (averaged from 1990 to 2002), about 80% of which falls between October and April during frequent, long-duration, low- to moderate-intensity frontal storms. The climate is Mediterranean with strong contrasts between summer and winter precipitation amounts [*Greenland*, 1994]. The catchment experiences a gradual wet-up period from about October to December and thereafter maintains very high wetness until late spring. Snow accumulations are common, but seldom persist longer than 1–2 weeks and generally melt within 1–2 days. No major snow accumulation was observed during this study. On average, 56% of the annual precipitation becomes runoff. Summer low flows are approximately 0.2 L s^{-1} (<0.01 mm h^{-1}) and typical winter storms obtain peak flows of approximately 40 L s^{-1} (1.4 mm h^{-1}). The largest storm on record produced a peak flow of 246 L s^{-1} (8.7 mm h^{-1}). The vegetation is dominated by a naturally regenerated second growth Douglas fir (*Pseudotsuga menziesii*) stand resulting from a 1975 clear-cut harvest.

[7] The catchment is steep with slopes ranging from 30 to over 45° and contains residual and colluvial clay loam soils (Typic Dystrocryepts) derived from andesitic tuffs (30%) and coarse breccias (70%) comprising the Little Butte Formation formed as the result of ashfall and pyroclasitic flows from Oligocene-Early Miocene volcanic activity [*Swanson and James*, 1975; *James*, 1978]. Average soil depth is approximately 130 cm. Surface soils are well aggregated with textures that vary from gravelly, silty clay loam to very gravelly clay loam; however, lower depths (70–110 cm) exhibit more massive blocky structure with less aggregation than surface soils [*Harr*, 1977; *Sollins et al.*, 1981]. Beneath the weakly developed A and B horizons is partially weathered parent material (saprolite) ranging in thickness from 1 to 7 m (~3.7 m on average) [*Harr and McCorison*, 1979; *Sollins and McCorison*, 1981].

[8] The catchment experiences periodic debris flows (e.g., as recently 1986 and 1996) that maintain a stream channel that is scoured to bedrock over the lower 60% of its length. The upper portion of the channel contains a narrow (<1 m), and in some cases, deeply incised near-stream area with frequent sections of exposed bedrock. In general, the channel width ranges from 0.25 m in the upper reaches to 1.0–1.5 m at the catchment's base [*Triska et al.*, 1984]. The overall slope of the stream channel is 24°. Thus, WS10 represents a catchment dominated by hillslopes with negligible storage of water in riparian sediments. Well-defined seeps have been identified flowing from the base of the hillslope soils into the stream channel [*Harr*, 1977; *Triska et al.*, 1984]. These seeps are highly localized zones of saturated soil related to the microtopography of the unweathered bedrock near the stream or to the presence of small vertical, andesitic dikes approximately 5 m wide, located within the basin [*Swanson and James*, 1975; *Harr*, 1977]. While the seepage areas remain isolated during and between events, we observed a linear increase in discharge downstream during a constant rate stream tracer experiment at low flow, suggesting a uniform contribution of hillslopes within the catchment.

[9] Our hillslope study area was located on the south aspect of WS10, 91 m upstream from the stream gauging
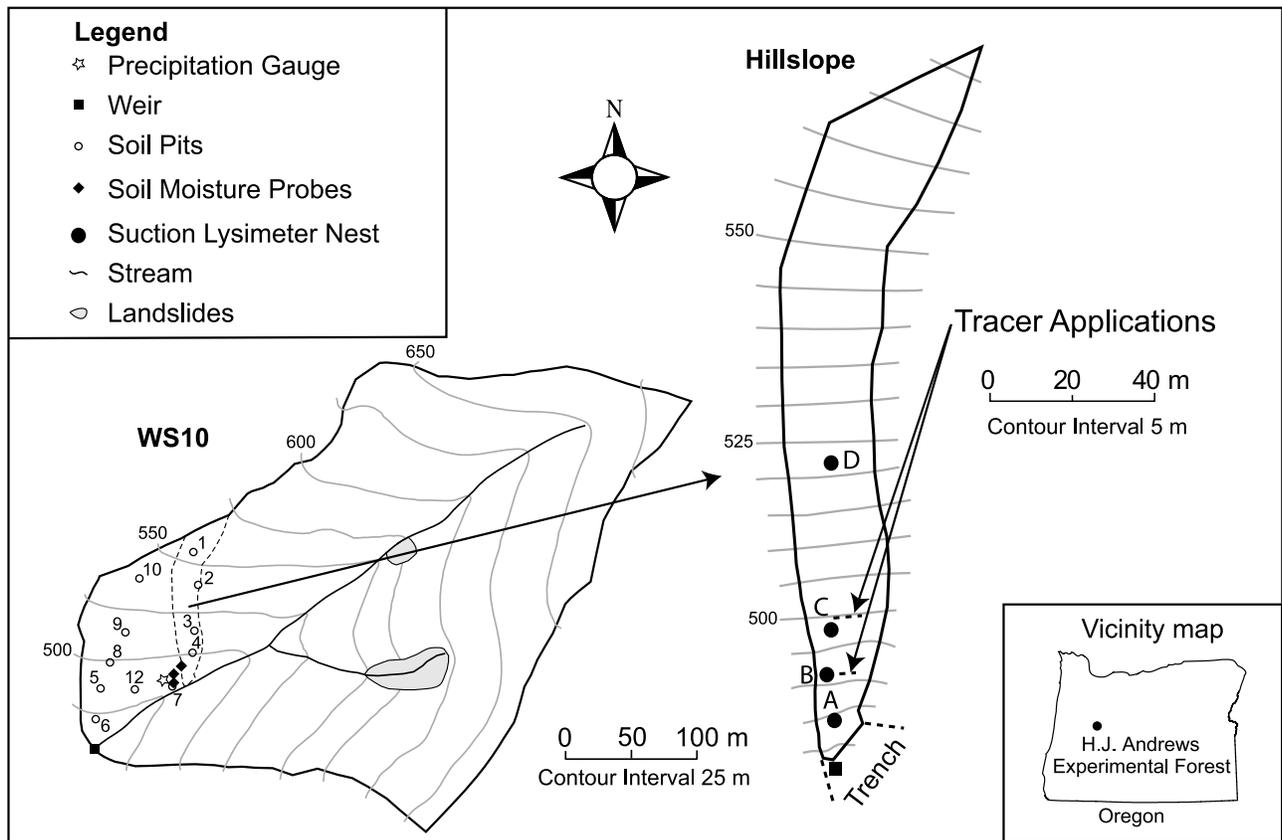
Figure 1. Map of WS10 showing the location of instrumentation and hillslope study area. THE WS10 weir is located at 44.2169°N and 122.2611°W, and the hillslope weir is located at 44.2175°N and 122.2589°W.

station (Figure 1) [*McGuire et al.*, 2007; *van Verseveld et al.*, 2009]. This site was reestablished from early 1970s era benchmark studies [*Harr and Ranken*, 1972; *Harr*, 1977; *Sollins and McCorison*, 1981; *Sollins et al.*, 1981]. The slope is representative of the two main planar hillslopes that compose the overall v-shaped catchment (WS10). The 125 m long stream-to-ridge slope is slightly convex and its gradient averages 37°, ranging from 27° near the ridge to 48° adjacent to the stream. Elevation ranges from 480 to 565 m. *Harr and Ranken* [1972] excavated eleven soil pits on the study slope (Figure 1) and collected 452 soil cores from the pits. The cores were analyzed for hydrologic properties including hydraulic conductivity, porosity, pore size distribution, moisture characteristics, and stone content [*Ranken*, 1974; *Harr*, 1977]. Hydraulic conductivity is sufficiently high that only the stream channel and bedrock surfaces produce overland flow. The main rationale for selecting this study slope was the richness of local data resources from these previous studies and the ability to be able to build on this knowledge base, specifically the studies by Harr and Ranken.

2.1. Instrumentation

[10] A 10 m long trench was constructed to measure subsurface throughflow at the location of a seep that had been previously gauged in the early to mid-1970s [*Harr*, 1977; *Triska et al.*, 1984]. The trench was constructed by intercepting subsurface water from a natural seepage face, which was routed to a calibrated 15° V notch weir that

recorded stage at 10 min time intervals using a 1 mm resolution capacitance water level recorder (TruTrack, Inc., model WT-HR). Discharge from the trench was measured from 1 September 2002 to 21 January 2003 and thereafter predicted using regression with WS10 discharge due to gauge failure. Precipitation was measured with a tipping bucket (15.39 cm diameter orifice, 0.2 mm resolution) and storage gauge (8.9 cm diameter orifice) observed on an event basis in a small canopy opening on the hillslope. The drainage area of the hillslope was delineated from a total station topographic survey of the entire hillslope (0.2 ha) and verified by a water balance calculation (i.e., compared similarly to the WS10 balance).

[11] Storm events were defined as periods of major rainfall separated by at least 24 h of rainfall intensities averaging less than 0.1 mm h^{-1}. Hydrographs for the trench outflow and WS10 flume were separated into quick flow (Q_F) and delayed flow using the *Hewlett and Hibbert* [1967] method by projecting a line with a constant slope of 0.55 L s^{-1} km^{-2} h^{-1} from the initiation of stormflow. The quick flow or the stormflow portion of the hydrograph was finally expressed as mm and runoff or quick flow ratios (Q_F/P) were calculated for each storm. Cumulative precipitation prior to each storm was summed over 7, 14, and 30 days (AP_7, AP_{14}, and AP_{30}) to represent antecedent conditions.

[12] Soil water content (θ) was measured using water content reflectometers (WCR) (CS615, Campbell Scientific, Inc.) installed horizontally at 3 depths (30, 70, and 100 cm)

in 3 soil pits in lower portion of the hillslope (Figure 1). The nests were located 15, 20 and 25 m from the slope base. The WCRs were calibrated using soil cores extracted from several locations at the H. J. Andrews, including WS10 [*Czarnomski et al.*, 2005; G. W. Moore et al., unpublished data, 2003]. No temperature effects were noted for the water content reflectometers under typical field temperature ranges [*Czarnomski et al.*, 2005]. Transient saturation in the soil profile was measured by 27 wells with short (15 cm) screened intervals instrumented with capacitance water level recorders (TruTrack, Inc., model WTDL 8000). Most of the wells were installed to bedrock; however, about a quarter of them were installed in the soil profile to depths where *Ranken* [1974] observed sharp saturated hydraulic conductivity contrasts. The capacitance water level recorders in the piezometers were only able to detect water levels >7.5 cm from the bottom of the well. Suction lysimeters were installed in fours nests along a hillslope transect (Figure 1). Each nest contained approximate 30, 70 and 90 cm depths, except site A, where bedrock was <90 cm deep.

2.2. Tracers

[13] Two line source tracers were applied to the hillslope immediately before a large winter rainstorm (66 mm, 49 h duration) that began on 9 December 2002 at 21:30 [see *McGuire et al.*, 2007]. 20.9 g of amino G acid monopotassium salt (AGA), a fluorescent dye [*Smart and Laidlaw*, 1977], and 4.0 kg of bromide (as LiBr solution) were applied 19 and 33 m from the trench, respectively. Both tracers were monitored continuously at the trench for the first 9 days of the experiment. AGA was monitored using a field fluorometer (10-AU, Turner Designs, Inc., Sunnyvale, CA) equipped with along wavelength optical kit, temperature compensation, flow-through cell, and data logger. Bromide was also measured in situ with an ion-selective electrode for Br^- (TempHion®, Instrumentation Northwest, Inc.) until 31 March 2003. Grab sampling extended the AGA breakthrough for 100 days and it provided additional samples for calibrating the Br^- selective electrode ($N = 107$, $R^2 = 0.99$). Both tracers were monitored until concentrations during storm events were at background levels (~100 days). Background concentrations of dissolved organic carbon can interfere with AGA fluorescence. Maximum observed background AGA concentrations reached about 10 $\mu g\ L^{-1}$ during an event in November 2002.

[14] Oxygen-18 (^{18}O) samples were collected weekly at the hillslope trench (1 November 2001 to 11 February 2003), WS10 (13 February 2001 to 4 February 2003), and as bulk precipitation (1 January 2000 to 11 February 2003). Soil water samples from the lysimeters were collected at time intervals between daily and weekly from 2 October 2002 until 11 February 2003. Storm samples were collected between 2 and 4 h intervals from the hillslope and WS10 for several storms during the fall 2002 to winter 2003 period. Rainfall was sampled sequentially (4.4 mm increments) over this period for ^{18}O using samplers as described by *Kennedy et al.* [1979]. All samples were analyzed at the USGS Stable Isotope Laboratory in Menlo Park, California using an automated version of the CO_2–H_2O equilibration technique of *Epstein and Mayeda* [1953]. The $\delta^{18}O$ values are reported in per mil (‰) relative to a standard as $\delta^{18}O = (R_x/R_s - 1) \times 1000$, where R_x and R_s are the $^{18}O/^{16}O$ ratios for the sample

and standard (VSMOW), respectively. The analytical precision (σ) was 0.11‰ on the basis of submitted blind duplicate samples.

2.3. Modeling

[15] Hydrograph separation and transit time models were used to quantify the proportions of event and preevent water and to estimate transit times of various runoff components within the hillslope and catchment. The TRANSEP (transfer function-hydrograph separation) model was used to estimate the event water contributions and transit time distributions [*Weiler et al.*, 2003; *Johnson et al.*, 2007; *Lyon et al.*, 2008, 2009; *Lyon and Troch*, 2010]. TRANSEP embraces the temporal event water signal and does not assume that rainfall instantaneously reach the stream (or hillslope trench). In conventional hydrograph separation models, bulk rainfall composition is used as the event water component, which can influence the separation during the early portion of an event by rain that has not yet fallen [e.g., see *McDonnell et al.*, 1990; *Pionke et al.*, 1993]. Instead, TRANSEP lags event water contributions according to an assumed transit time distribution (TTD) and thus more realistically represents the nature of event water contributions [*Joerin et al.*, 2002; *Laudon et al.*, 2002; *Renshaw et al.*, 2003; *Weiler et al.*, 2003; *Lyon et al.*, 2008]. In this study, we used two different TTDs: a two parallel linear reservoir model and a gamma model depending on which model best fit the $\delta^{18}O$ data and had identifiable parameters (see *Weiler et al.* [2003] for additional details regarding the model).

[16] We examined the transit time of soil water within several slope positions, hillslope runoff, and stream base flow using a lumped parameter convolution model to interpret observed $\delta^{18}O$ variations [*Stewart and McDonnell*, 1991; *Murray and Buttle*, 2005; *McGuire and McDonnell*, 2006]. The transit time models predict output $\delta^{18}O$ (i.e., soil water, seepage, or stream flow) as a weighted sum of the past $\delta^{18}O$ input composition. The weighting function or transit time distribution (TTD) describes the time it takes water to travel from the ground surface to an outflow location (soil water, seepage, or stream flow). The TTD that gives the best fit between observed and simulated output $\delta^{18}O$ is assumed to represent the flow system [*McGuire and McDonnell*, 2006].

[17] The transfer of approximately three months of daily $\delta^{18}O$ inputs into the soil was described using a TTD representing a one-dimensional solution to the advection-dispersion equation under volumetrically sampled conditions for a semi-infinite medium [*Kreft and Zuber*, 1978; *Stewart and McDonnell*, 1991]. This TTD was selected because shallow soil water flow at this site is largely vertical [see *Harr*, 1977]. The transit time model for WS10 is discussed elsewhere [*McGuire et al.*, 2005]; however, it generally follows the same approach as the soil water transit time models, except that an exponential distribution was used for the TTD. The hillslope transit time was estimated using the same method as WS10.

3. Results

3.1. Threshold Runoff Response

[18] A series of 18 storms were monitored during the wetup phase of the 2002–2003 winter rainy season (Table 1 and

Table 1. Storm Characteristics for Events During the Fall 2002 to Winter 2003 Wet-Up Period

| | Beginning of Precipitation | | | | | | | Quick Flow Ratio[b] Q_F/P | |
	Date	Local Time	Duration (h)	Gross Precipitation[a] (mm)	30 min Maximum Intensity (mm/h)	Antecedent Precipitation, 14 day (mm)	Antecedent Precipitation, 30 day (mm)	Hillslope	WS10
Storm 1	16 Sep 2002	1810	25	23	4.1	9	0	NA	NA
Storm 2	29 Sep 2002	0750	44.2	29	5.6	23	0	NA	NA
Storm 3	3 Oct 2002	0910	15.5	13	3.6	29	52	NA	NA
Storm 4	7 Nov 2002	1230	107.5	177	7.6	19	19	0.02	0.03
Storm 5	16 Nov 2002	1000	61.8	31	6.1	177	179	0.04	0.07
Storm 6	9 Dec 2002	2130	49.5	66	6.6	33	101	0.10	0.15
Storm 7	12 Dec 2002[c]	1450	94	96	6.1	85	140	NA	NA
Storm 8	20 Dec 2002	0230	82.5	60	7.1	168	180	0.23	0.21
Storm 9	29 Dec 2002	2100	88.3	79	5.1	194	310	0.42	0.41
Storm 10	2 Jan 2003	0530	60.2	66	6.6	225	392	0.14	0.36
Storm 11	11 Jan 2003	0320	79.8	51	6.6	186	425	0.23	0.19
Storm 12	21 Jan 2003[d]	1100	40.2	23	8.6	51	282	0.03	0.05
Storm 13	24 Jan 2003	0150	83.8	98	6.6	74	304	0.33	0.44
Storm 14	29 Jan 2003	0710	148.3	152	8.6	121	312	0.38	0.56
Storm 15	15 Feb 2003	1100	170	140	5.1	15	282	0.16	0.25
Storm 16	5 Mar 2003	0210	307	230	7.1	81	174	0.40	0.61
Storm 17	19 Mar 2003	1330	100.2	126	4.1	247	352	0.33	0.49
Storm 18	24 Mar 2003	2000	68.8	84	7.6	173	412	0.31	0.47
Mean								0.22	0.31

[a]Storm events are defined as periods of major rainfall separated by at least 24 h of rainfall intensities averaging <0.1 mm/h.

[b]Quick flow ratios (Q_F/P) were determined by projecting a linear 0.55 L s^{-1} km^{-2} h^{-1} slope from the onset of storm runoff [*Hewlett and Hibbert*, 1967]. Q_F/P is shown as not applicable (NA) if the separation was not possible or if Q_F/P is greater than calculated channel interception for WS10.

[c]A complex low rainfall intensity storm and hydrograph occurred during this period.

[d]From this date onward, hillslope discharge was predicted from a regression equation using WS10 due to gauge failure.

Figure 2). Three distinct phases can be seen in Figure 2: (1) a dry period when soil moisture was steady, (2) an intermediate transition when soil moisture responds to precipitation and when base flow increased at both the hillslope and WS10, and (3) a wet period when base flow levels of soil moisture, hillslope outflow, and WS10 discharge all increased and maintained higher levels.

[19] Gross precipitation amounts ranged from 13 to 230 mm with 30 min maximum intensities of 9 mm h^{-1}. During the early part of this period, several fall storm events caused small responses in both hillslope and WS10 runoff (storms 1 to 3). The storm runoff for these events for WS10 could be explained entirely by channel interception of storm rainfall (i.e., on the basis of measurements of bankfull width at 10 m intervals, 767 m^2). However, a hillslope runoff response was observed for each of these events indicating that a small portion of the hillslope contributed to storm-flow even though soil moisture response was negligible. One exception to this was a <2 mm rain burst on 27 October (Figure 2), where only WS10 responded to channel interception inputs and hillslope runoff remained constant.

[20] Hillslope seepage was sustained throughout the dry fall period (i.e., from 1 September to 1 November) and constituted about 15% of the discharge on a volumetric basis at the WS10 outlet. Hillslope contribution to WS10 volumetric discharge dropped dramatically after a major storm on 7 November to an average contribution of approximately 2% of WS10 for the remainder of the study. The transition period, beginning with storm event 4, signified the initial soil moisture response on the hillslope (Figure 2) and the first event with a determinable Q_F. The hillslope Q_F was 3.5 mm and WS10 Q_F was 5.3 mm. Q_F/P generally increased through time after this event (Figure 3a) with total storm precipitation explaining most of the temporal variance. Quick flow was not

produced at either the trench or catchment for rainfall amounts less than 30 mm. Antecedent precipitation, as the 14 day cumulative precipitation prior to a storm (AP$_{14}$), did not appear to significantly influence the observed near linear relationship between rainfall amount and hillslope quick flow that occurred after the 30 mm threshold (Figure 3b). The exception to this was when the AP$_{14}$ was less than 20 mm, and then the values plotted below the overall trend (Figure 3b). Otherwise, quick flow ratios for WS10 exceeded 30% when total storm precipitation was greater than about 65 mm. Other AP indices (e.g., 7 or 30 day) did not describe the nature of the rainfall-Q_F relationship any better than AP$_{14}$.

[21] Some insight into the threshold hillslope processes can be obtained through analysis of soil moisture dynamics (θ) within the hillslope. Soil moisture at 30 cm responded relatively quickly to rainfall, reflecting a primarily vertical infiltration wetting front. There were no apparent differences in response times of shallow θ measurements between the three slope positions. In contrast, θ measured at 100 cm in the soil profile at all three positions exhibited marked time lags compared trench outflow (Figure 4) and were correlated to Q_F/P (r = −0.66 to −0.70, p value < 0.04).

[22] The first storm with an observable θ response at the 100 cm depth was event 5, which responded 1 to 19 h after the peak of hillslope throughflow (Figures 2 and 4). However, the soil moisture sensor located at the upper site at 100 cm depth showed no response to this event, while the midposition 100 cm depth lagged the seepage response more than the lower site. Storm 6, which occurred on 9 December, increased WS10 base flow by more than an order of magnitude and shifted θ to levels that were maintained throughout the rest of the winter period (wet phase, Figures 2 and 4). Thereafter, soil moisture responses at all
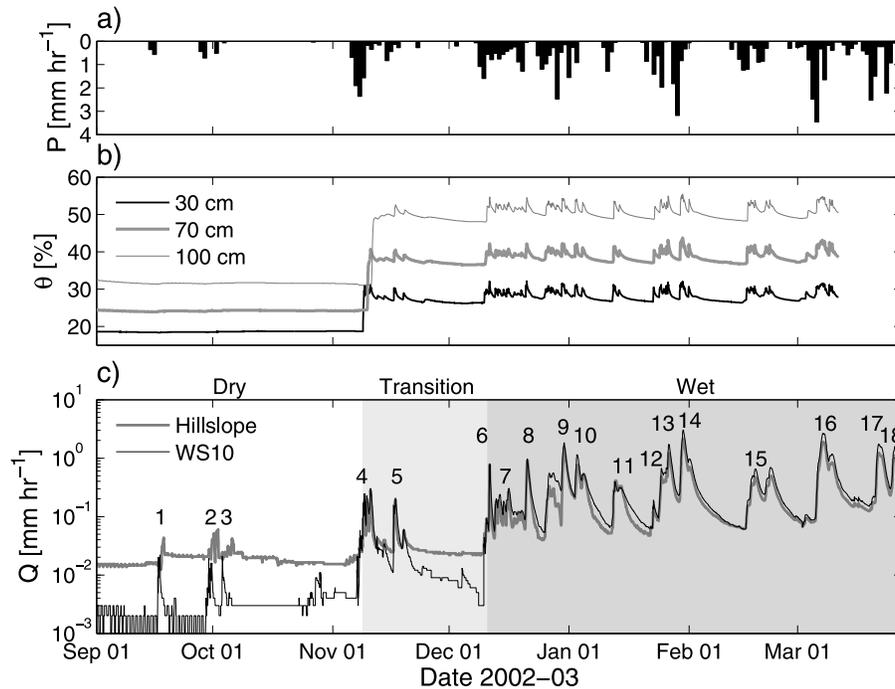
Figure 2. Time series of the hydrologic conditions of the study period: (a) precipitation, (b) volumetric water content (θ) from the lower nest of water content reflectometers, and (c) discharge from the hillslope and catchment. The shading indicates the wetting phases during this study period: the dry period is characterized by no soil moisture response, the transition period corresponds to an increase in hillslope soil moisture and stream base flow, and the wet period represents elevated base flow conditions and approximate synchronization between hillslope and stream discharge. The numbers in Figure 2c identify storms that are referred to in the text and in Table 1.

sites were nearly synchronized with the hillslope peak runoff (Figure 4). Soil moisture responses generally peaked prior to the hillslope peak runoff by approximately 5 h. The general order of soil moisture response for each hillslope position began with the lower site and became more delayed for each upslope site, which suggested that the hillslope wetted up from the bottom (Figure 4). While saturation was not directly observed using the soil moisture sensors at any time during this study (i.e., θ did not plateau), observed values of θ at 100 cm during storms between events 8 and 11 indicated soils reached near saturation. Soil moisture content at the lowest site was generally higher compared to the upslope positions.

[23] During the winter period when antecedent wetness was high, soil moisture at 100 cm depth lagged rainfall intensities (defined as the time of mass center) on average by 0.3, 0.3, and 0.5 h for the lower, middle, and upper slope water content reflectometers (WCRs), respectively, indicating a rapid moisture response in the lower soil profile. Estimated vertical fluxes for the two upper WCRs (i.e., the 10 and 30 cm sensors) exceed saturated hydraulic conductivity (reported by *Ranken* [1974]) by approximately a factor 10 (average soil profile $K_{sat} \approx 45$ cm h^{-1}).

[24] No saturated zones were detected by any of the wells during the study period. While our observations were limited by the number of wells we deployed (27) and the water level recorder detection limit (7.5 cm), it is striking that transient water tables were not observed. Thin saturated zones (<5 cm) were periodically observed at the bedrock-

soil interface in wells located above the seep and in other near-stream wells that were used for sampling water during storms.

3.2. Hillslope-Catchment Runoff Hysteresis

[25] Stormflow from the hillslope and WS10 with a determinable Q_F/P were examined in sequence (commencing after the 3 month summer dry period, Figure 2) to understand the timing of hillslope contribution and hillslope-stream coupling through the wet-up period. Figure 5 shows the temporal dynamics of hillslope and stream coupling during our study period. During the first event with a measurable Q_F/P (storm 4), the hillslope and stream were synchronized through the entire 3 day storm event, which had low Q_F/P values of 2 and 3% for the hillslope and WS10, respectively. Four days later, another storm occurred approximately doubling Q_F/P, during which the hillslope discharge led the WS10 hydrograph revealing a hysteretic relationship between the two runoff responses. This effect became more pronounced during storm 6 when Q_F/P was 10 and 15% for the hillslope and WS10, respectively.

[26] The hillslope and WS10 were completely synchronized and contributed equal unit area discharge to the storm hydrograph throughout storm 8 (Figure 5). Interestingly, during storm 9, the hysteresis pattern reversed. This occurred when Q_F/P was at the highest observed value for the hillslope and again doubled Q_F/P of the previous storm event (see Table 1). Also during this period, the time lag between peak soil moisture response and hillslope discharge was
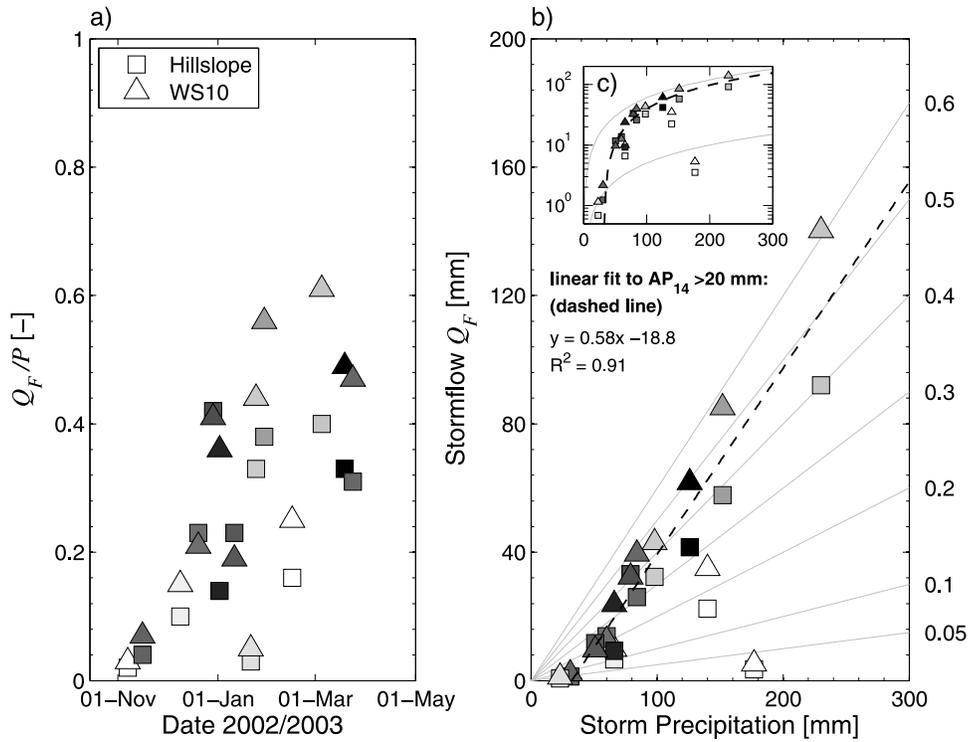
Figure 3. (a) Quick flow ratios (Q_F/P) over time and (b) total storm precipitation and stormflow (as per *Hewlett and Hibbert* [1967]) relationships for the hillslope (squares) and WS10 (triangles). The gray scale for the symbols indicates relative antecedent precipitation (AP_{14}), and white symbols are storms that occurred when $AP_{14} < 20$ mm. Sloping gray lines show quick flow (Q_F/P) ratios, which are labeled next to the right axis. (c) Logarithmic expansion of the y axis of Figure 3b, which includes gray reference lines for $Q_F/P = 0.05$ and 0.6. A linear fit (dashed line) to storms with $AP_{14} > 20$ mm with a slope 0.58 is shown in Figures 3b and 3c.
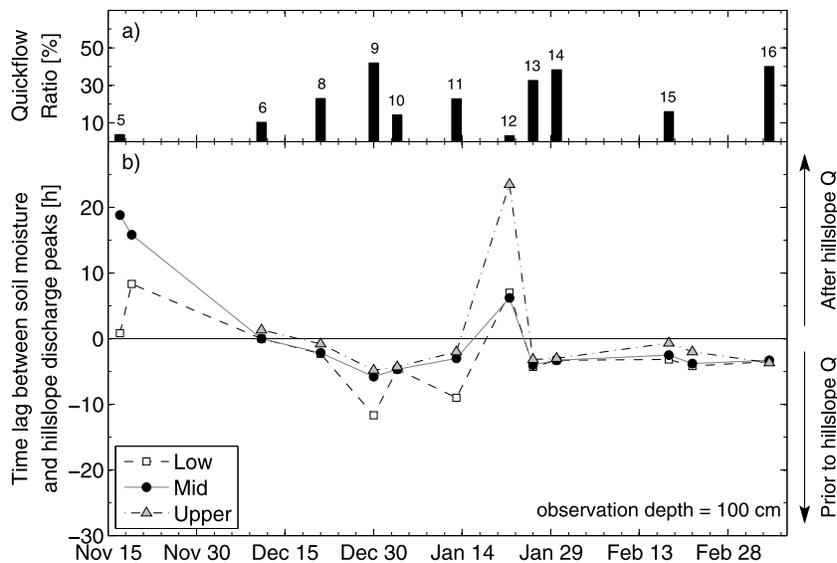
Figure 4. (a) Quick flow ratios for storms 5–16 observed at the hillslope trench and (b) soil moisture time lags compared to the hillslope runoff measured at the trench. Soil moisture measurements were recorded from sensors at 100 cm depth from the transect above the trench at lower (squares), middle (circles), and upper (triangles) slope positions representing 15, 20, and 25 m from the slope base, respectively. Soil moisture time lags >0 indicate peak responses *after* the peak of the outflow measured at the trench downslope, and time lags <0 indicate peak responses *before* the peak of the hillslope outflow.
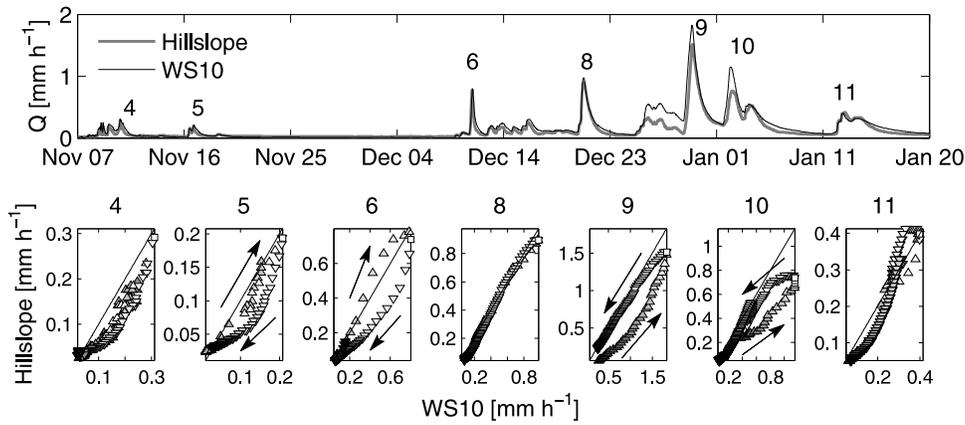
Figure 5. Temporal changes in the relationship between hillslope and catchment runoff through the wet-up period: (top) time series of the continuous discharge data with enumerated storms that identify (bottom) the scatterplots. Triangles indicate the rising limb of the WS10 hydrograph, and inverted triangles indicate the falling limb. The gray scale for the symbols shows the time sequence to and from the WS10 peak flow (square).

greatest (soil moisture responses peaked 5 to 10 h prior to the discharge peak) (Figure 4). Q_F/P for WS10 decreased slightly for the next storm (storm 10) to 36% and the hillslope-WS10 discharge pattern remained anticlockwise. As Q_F/P decreased back to values similar to storm 8, the relationship began to approach the clockwise hysteresis pattern again (storm 11). Comparison between the hillslope and WS10 was not possible after storm 11, since the hillslope runoff gauge failed after that storm.

3.3. Hillslope Tracer Response

[27] We applied tracers 19 and 33 m from the trench to test the degree of connectivity between the hillslope and stream as suggested by the hydrometrics and determine potential mode of transport (matrix or preferential flow)

in our hillslope soils [*McGuire et al.*, 2007]. Tracers were applied prior to a major rainfall event that began on 9 December 2002 at 21:30 (defines the start of the experiment and $t = 0$ for the timing of tracer and soil moisture response). Tracer breakthrough was extremely rapid and almost identical for both tracers even though Br$^-$ was applied 14 m farther upslope than AGA (Figure 6). Tracer concentrations peaked 40.4 and 40.3 h after the start of rainfall, for AGA and Br$^-$, while the time of midrise on the breakthrough curve was 37.3 and 38.4 h for AGA and Br$^-$, respectively. Peak soil moisture from the two lower slope positions and peak hillslope throughflow all occurred 38.8 h from $t = 0$, while peak soil moisture from the upper site coincided with the peak breakthrough concentrations (40.2 h). This suggests that a continuous hydrologic connection of near-saturated
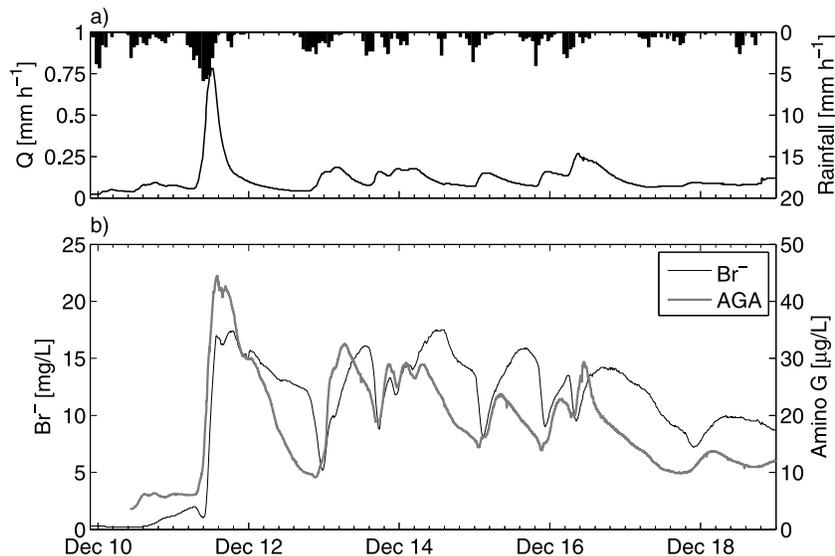
Figure 6. (a) Hillslope rainfall and runoff measured by the throughflow trench. (b) Tracer breakthrough curves of bromide (Br$^-$) and amino G acid (AGA), which were applied as line source additions 33 and 19 m, respectively, from the hillslope throughflow trench.
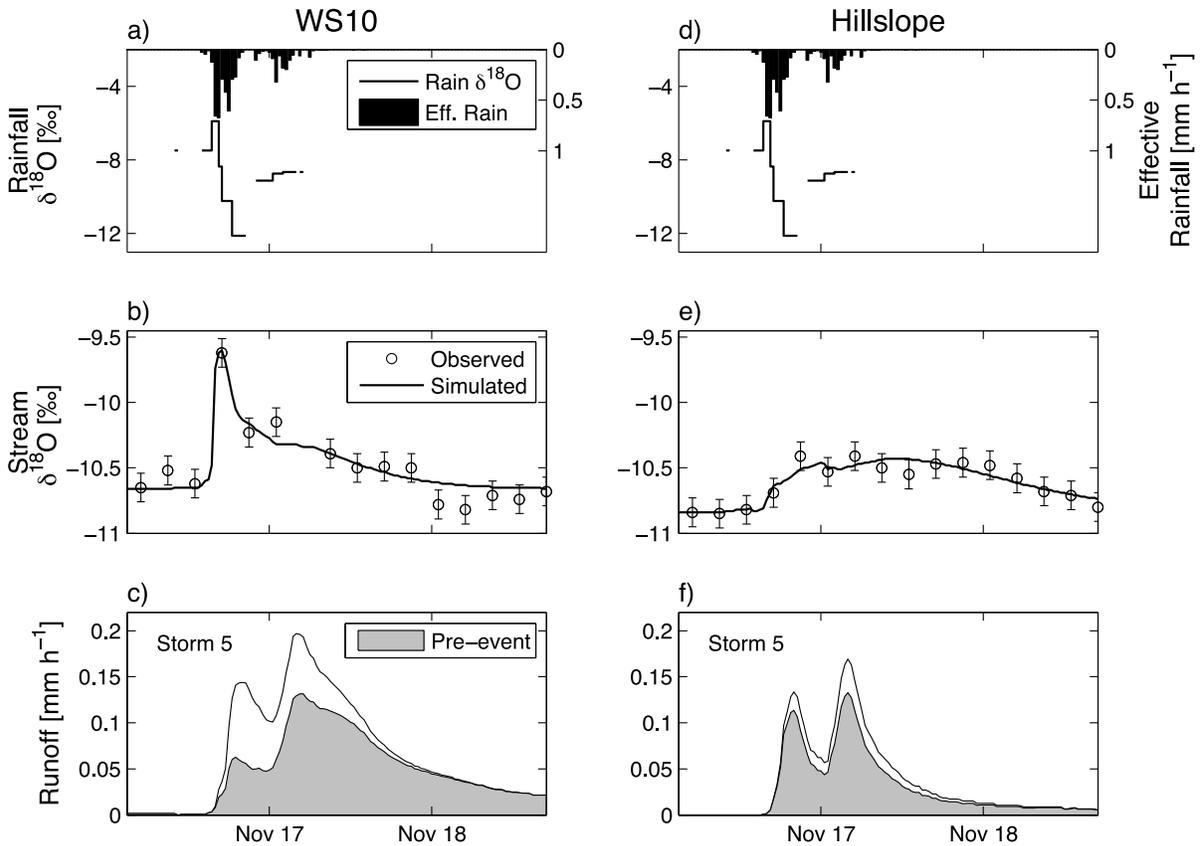
Figure 7. TRANSEP isotope hydrograph separations for storm 5 for (left) WS10 and (right) the hillslope. (a and d) Shown are rainfall $\delta^{18}O$ (left axis) and effective rainfall amounts (right axis) that contribute to stormflow [see *Weiler et al.*, 2003]. Note that both sites received the same precipitation isotopic composition. Also shown are the observed and simulated $\delta^{18}O$ for (b) WS10 and (e) hillslope. The error bars represent $\delta^{18}O$ analytical precision (0.11‰). (c and f) Hydrograph separations, shown by the shaded region.

soils occurred on the lower 25 m of hillslope at ~40 h during this storm. In addition, the response times indicate that subsurface flow velocities were between 0.47 to 0.51 m h^{-1} and 0.82 to 0.86 m h^{-1} for the AGA and Br$^-$, respectively, and are thus capable of transporting water over at least this slope distance.

[28] During the first 10 days of the experiment, both AGA and Br$^-$ concentrations were high and responsive to rainfall with smoother Br$^-$ concentrations indicating greater dispersion of the line source applied further upslope compared to the AGA tracer applied lower on the slope (Figure 6). After this period, the concentrations began to slowly recede. Overall, 19 and 53% of the applied tracer mass was recovered for AGA and Br$^-$, respectively, after 100 days of monitoring when tracers reached background levels. Due to difficulties in quantifying background concentrations [see *Smart and Laidlaw*, 1977], the AGA recovery is uncertain and likely overestimated. Nevertheless, this does not affect the finding of coincident breakthrough, since AGA concentrations were at least 4 times greater than potential background concentration estimates at the peak breakthrough time.

3.4. Event Water Contributions

[29] The fraction of event water comprising the hydrograph at peak flow was generally less than 30% (Table 2). On the basis of only two storms, the fraction of event water decreased with larger stormflow contribution (i.e., Q_F/P) for both the hillslope and stream (Table 2). The rainfall isotopic composition varied significantly through the storm periods (Figure 7), which led to high uncertainties [*Genereux*, 1998] using conventional isotope hydrograph separation methods [*Sklash*, 1990; *Buttle*, 1994]. For that reason, and to extract more information from the isotope record of these storms, the TRANSEP modeling approach was used. In the example TRANSEP simulation shown in Figure 7, it is clear that the hillslope and catchment responded differently to the same $\delta^{18}O$ rainfall input. The hillslope tracer response was lagged and considerably damped compared to the stream signal even though the hillslope runoff recessions decreased more rapidly. Generally, event water contributions were lower at the hillslope compared to WS10 (Table 2). Figure 8 shows the event water transit time distributions (TTDs) for two hillslope storms (events 5 and 8) and three WS10 storms (events 4, 5, and 8). These were obtained by a fitting pro-

Table 2. Isotope Hydrograph Separation Results

Storm	Date	Model[a]	Number of Runoff δ^{18}O Samples	MTT[b] (h)	Peak Flow Event Water (%)	Mean Event Water (%)	Model Efficiency[c]	Mean Absolute Error (‰)
Hillslope								
Storm 5	16 Nov	Gamma	14	15	13	22	0.85	0.04
Storm 8	20 Dec	TPLR	38	14	9	6	0.48	0.18
WS10								
Storm 4	7 Nov	TPLR	50	28	11	11	0.78	0.13
Storm 5	16 Nov	Gamma	13	8	34	27	0.90	0.07
Storm 8	20 Dec	TPLR	40	34	15	10	0.50	0.16

[a]Event water transit times were estimated using the TRANSEP model [*Weiler et al.* 2003].
[b]Mean transit time (MTT) is calculated numerically from a multiparameter transfer function.
[c]Nash-Sutcliffe efficiency [*Nash and Sutcliffe*, 1970].

cedure; goodness-of-fit statistics are shown in Table 2 along with the estimated mean transit times (MTT) of event water. Estimated MTTs ranged from 8 to 34 h. Hillslope event water contribution was lagged considerably compared to WS10 for storm 5 (Figures 7 and 8), with slightly lower event water proportions (22 and 27% for hillslope and WS10 mean event water contribution, respectively).

3.5. Soil Water, Hillslope Runoff, and Catchment Transit Times

[30] Event water percentages represented a minor portion (<30%) of the overall runoff. Thus, the origin of the pre-event water fraction, which dominates the hydrograph during wet and dry conditions, is of greater interest for understanding how hillslopes are linked to their streams. Figure 9 illustrates an example data set and simulation for one of the suction lysimeters (D70). The marked rainfall and soil water ^{18}O depletion that occurred during mid-December (Figure 9) allowed for high modeling efficiencies (Table 3). The soil water MTTs are conservatively high estimates, since the time associated with each sample was the end of the collection period, which would tend to attenuate the δ^{18}O signal of preferential flow that may have been collected in the suction lysimeters. The TTDs for each lysimeter are shown in Figure 10. Estimated mean transit times for shallow soils (30 cm) were approximately 13 days, while deeper soils (70 and 90 cm) were 22 days. Dispersion was inversely correlated to lysimeter depth (Figure 10 and Table 3) (r = −0.73, p value = 0.011) and MTT estimates were positively correlated to lysimeter depth (r = 0.87, p value = 0.001), but there was little correlation with lysimeter slope distance or distance to the stream (r = 0.45, p value = 0.177). The estimated MTTs were slightly less than turnover times calculated from a water balance. Total rainfall over the lysimeter collection period (~90 days) was about 900 mm and the average water content for the upper meter of soil was about 33% (storage ≈ 300 mm). Therefore, assuming steady state conditions, the turnover time for 90 cm of soil would be approximately 30 days (90 days/[900 mm/300 mm] = 30 days). MTTs determined from the isotope analysis seem reasonable, but indicate some contribution of more rapid pathways than the water balance estimate might suggest. Both estimates imply that more than 2 pore volumes were replaced within the soil over our study period and suggest that most of the soil water was mobile.

[31] Catchment and hillslope water transit times were significantly longer than soil water MTTs. MTTs estimated

for WS10 and the hillslope were 1.2 and 1.8 years, respectively (Table 3). Exponential TTDs were assumed to represent the spatial integration of flow paths at the catchment and hillslope scales. These values were determined from models representing nonstorm conditions and thus, largely reflect base flow conditions. Transit times estimated for WS10 and other basins in the HJA showed no correlation to catchment area, but were strongly correlated to median flow path length and gradient determined from topographic analyses, indicating the importance of hillslope contributing areas (for detailed discussion of these data, see *McGuire et al.* [2005]). While the estimated MTT for the hillslope was 0.6 years longer than its catchment (WS10), parameter uncertainty (Table 3) suggests that the values are indistinguishable, especially considering that about 35%
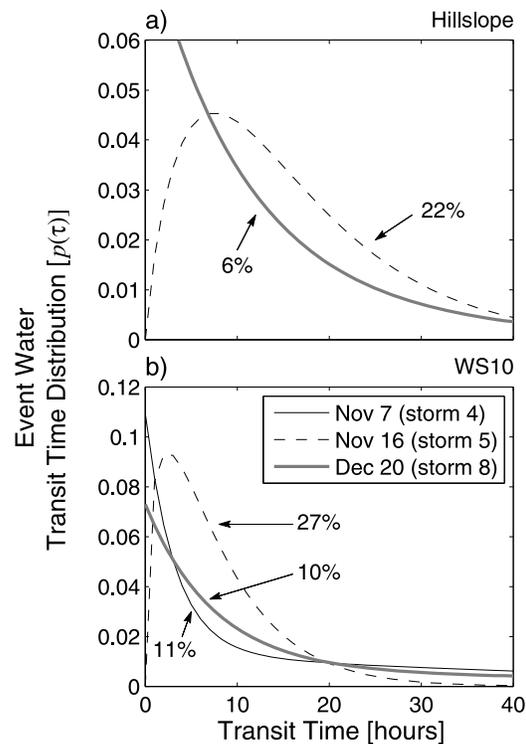
Figure 8. Event water transit time distributions for storms 4, 5, and 8 for (a) the hillslope and (b) the catchment. Mean event water percentage are shown for each storm (see Table 2).
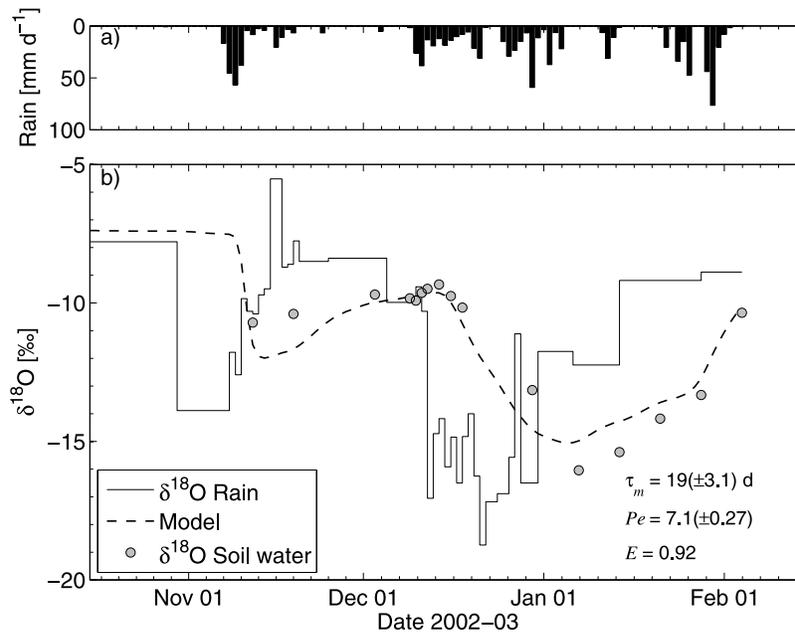
Figure 9. (a) Daily rainfall and (b) an example $\delta^{18}O$ simulation for lysimeter D70 modeled using a one-dimensional advection-dispersion model. The mean transit time (τ_m) for this simulation is 19 (± 3.1) days with a Peclet number, Pe, ($1/D_p$) of 7.1 (± 0.27) (i.e., a fitting parameter describing ratio of advective to dispersive time scales). The Nash-Sutcliffe efficiency [*Nash and Sutcliffe*, 1970], E, is 0.92. The analytical precision of $\delta^{18}O$ (0.11‰) is less than the size of the plotted circle for soil water $\delta^{18}O$.

fewer samples were collected from the hillslope compared to WS10 (i.e., hillslope sample collection began later in study).

4. Discussion

[32] We have described factors that control hydrologically the connection between hillslopes and streams. Previously, much of the difficulty in deciphering hillslope response in the stream is due to the riparian zone modulation of these inputs. Our use of watershed 10 at the H. J. Andrews Experimental Forest enabled a natural experimental design that provided an explicit and unambiguous hillslope hydrologic signal to the stream channel. Our approach using combined hydrometric, stable isotope, applied tracer and computed transit times allowed to decipher the physical controls on runoff generation and hillslope-stream connectivity on this hillslope.

[33] We reject hypothesis 1 that the hillslope runoff is linearly related to the catchment runoff. Our results showed clearly there are hysteretic effects that dominate hillslope-stream connectivity at our site. In addition, a threshold response between precipitation and stormflow was observed for both the hillslope and catchment. We also reject hypothesis 2 that hillslopes are not capable of transporting solutes (tracer) to the stream from upslope areas over the time scale of a storm event. Our measured subsurface velocities were between about 0.5 and 0.8 m h^{-1} and show clearly, transport over significant length scales (>80 m) that occur over the time scales of typical events (e.g., 100 h). We reject hypothesis 3 that event water contributions are similar for the hillslope and catchment. Hillslope event water ratios were consistently less than catchment values and mean

transit times were different between the hillslope and catchment with no apparent patterns in their magnitude. Finally, we reject hypothesis 4 that hillslope transit time increases downslope and is similar to the stream when it reaches the slope base. Transit times in the soil varied only with depth vertically in the profile, on the order of 15 to 25 days. Measured transit times for flow at hillslope and at the catchment outlet were on the order of 1–2 years, suggesting deep flow contributions. Below we explore the how these findings relate to past work at our site, help to describe the nature and extent of hydrologic connectivity at our site, and result in a new conceptual model for hillslope-stream connectivity based on transit times.

4.1. Nonlinear Hillslope Contributions: An Update to *Harr* [1977]

[34] The nature of hillslope runoff initiation was not studied by *Harr* [1977], since field observations were made during only winter conditions when the hillslopes were already producing runoff. *Harr* [1977] focused on the hydrometric characterization of subsurface stormflow in WS10 during wet winter conditions. The major findings from that study that relate to this work were (1) subsurface saturated areas expanded upslope and generally persisted over the lower 12–15 m of the hillslope, (2) transient saturation occurred at midslope to upslope locations at the soil-saprolite interface (persisted for <20 h), (3) subsurface fluxes in these saturated zones were high (i.e., 10–25 cm h^{-1}) in midslope to upslope locations if connected to the more permanently saturated zones at the based of the slope, (4) unsaturated flow dominated over all but the lower 12–15 m of the hillslope with water flux directed more laterally downslope

Table 3. Mean Transit Times for Soil Water and Base Flow at the Hillslope and Catchment Scales

Sampler Identification[a]	Model[b]	MTT[c]	D_p[d]	Model Efficiency[e]	Mean Absolute Error (‰)
Soil Water[f]					
A30-1	DM	14 (±4.6)	0.24 (±0.17)	0.85	0.71
A30-1	DM	14 (±6.6)	0.29 (±0.31)	0.80	0.83
A32	DM	10 (±2.8)	0.18 (±0.10)	0.86	0.86
A34	DM	12 (±3.0)	0.19 (±0.11)	0.86	0.81
A70	DM	22 (±3.3)	0.08 (±0.07)	0.89	0.63
B30	DM	12 (±3.2)	0.17 (±0.10)	0.83	0.82
B70	DM	24 (±1.8)	0.03 (±0.01)	0.80	0.88
B95	DM	20 (±2.2)	0.08 (±0.04)	0.94	0.43
C30[g]	–	–	–	–	–
D30	DM	16 (±2.2)	0.08 (±0.04)	0.93	0.46
D70	DM	19 (±3.1)	0.14 (±0.07)	0.92	0.45
D92	DM	25 (±2.8)	0.03 (±0.02)	0.72	0.57
Base Flow					
Hillslope	EM	1.8 (±0.43)		0.67	0.08
WS10[h]	EM	1.2 (±0.29)		0.49	0.15

[a]Sampler identification, designated as A, B, D, and D for lower, midlower, midupper, and upper relative slope positions (see Figure 1) with sampling depth (cm) indicated by the number (e.g., A32 = lower slope position at 32 cm depth).

[b]DM, dispersion model of transit times; EM, exponential model of transit times.

[c]Mean transit time (MTT) in months or years for soil water and base flow, respectively. Values in parentheses indicate $\pm 2\sigma_p$, as an approximation of the 95% confidence limit.

[d]Dispersion parameter (D_p) for soil water. Values in parentheses indicate $\pm 2\sigma_p$ as an approximation of the 95% confidence limit.

[e]Nash-Sutcliffe efficiency [*Nash and Sutcliffe*, 1970].

[f]Based on the approach of *Stewart and McDonnell* [1991].

[g]No suitable model was found to fit the data.

[h]From *McGuire et al.* [2005].

during storms and vertically between storms, and (5) streamflow responded to rainfall inputs prior to hillslope response.

[35] More recent studies on steep hillslopes elsewhere have also shown the importance of unsaturated flow [*McDonnell*, 1990; *Wilson et al.*, 1991; *Torres et al.*, 1998], the perching of transient saturated zones at soil-bedrock or saprolite interfaces [*Hammermeister et al.*, 1982; *Woods and Rowe*, 1996; *Freer et al.*, 2002; *Buttle*, 1994], and the modulation of subsurface water fluxes between vertical and lateral directions between and during storms, respectively [*Hoover*, 1985; *Jackson*, 1992].

[36] Even though saturation (>7.5 cm) in the soil profile was not directly measured in our study, it was periodically observed during wet conditions (Figure 2) in nonrecording wells and suggested by the high soil water content measured at 100 cm depth. Maximum saturated thickness observed by Harr (HJA LTER program and Forest Science Data Bank-HF01, unpublished data, 1975) and *van Verseveld* [2007] never exceeded 25 cm in the soil profile during similar types of events, indicating only thin zones of saturation developed during wet, storm conditions in these very high drainable porosity soils. The location of saturation development occurred over the low hydraulic conductivity saprolite or bedrock [*Ranken*, 1974; *Harr*, 1977].

[37] In our study, we measured hillslope runoff from dry to wet conditions and found a threshold rainfall amount was necessary to initiate hillslope runoff and thus establish a hillslope-stream connection. While rainfall events of less

than 30 mm generated some streamflow in WS10, those events did not generate significant subsurface stormflow at the trenched hillslope. Instead events <30 mm that occurred through the fall period, contributed to soil water recharge reducing soil water deficits. Threshold stormflow effects that occur after about 20 mm rainfall have been also observed in other humid Pacific Rim studies [*Mosley*, 1979; *Sidle et al.*, 1995; *Tani*, 1997] and elsewhere [*Whipkey*, 1965; *Peters et al.*, 1995; *Buttle et al.*, 2004]. In our work, like many of the other published studies, antecedent wetness appears to play a secondary role in terms of this threshold rainfall amount. Our antecedent wetness control appears to be at the seasonal time scale, linked to the broad wet then dry season dynamics.

[38] The striking hysteresis patterns between hillslope and catchment runoff reveal greater complexity in how hillslope runoff contributes to streams than was suggested by *Harr* [1977]. Harr and other investigators [e.g., *Weyman*, 1970, 1973; *Turton et al.*, 1992; *McGlynn et al.*, 2004] have found that hillslope runoff is often delayed compared to streamflow. This might suggest that hillslope subsurface flow results from transient saturated conditions that develop after soil moisture deficits are filled causing the peak of hillslope runoff to follow that of the stream. Our results show a more complex interaction between the hillslope and catchment runoff through a range of high-frequency changes in antecedent conditions. During the transition phase (Figures 2 and 5), the hillslope leads the WS10 hydrograph and contributes a greater proportion of flow on the rising limb of the WS10 hydrograph. As antecedent wetness increases, the hysteresis pattern is reversed (Figure 5). While some studies have shown that hillslope runoff can peak prior to streamflow [*Peters et al.*, 1995; *Kim et al.*, 2004] and others have shown that hillslope runoff peak at the time of peak stream-
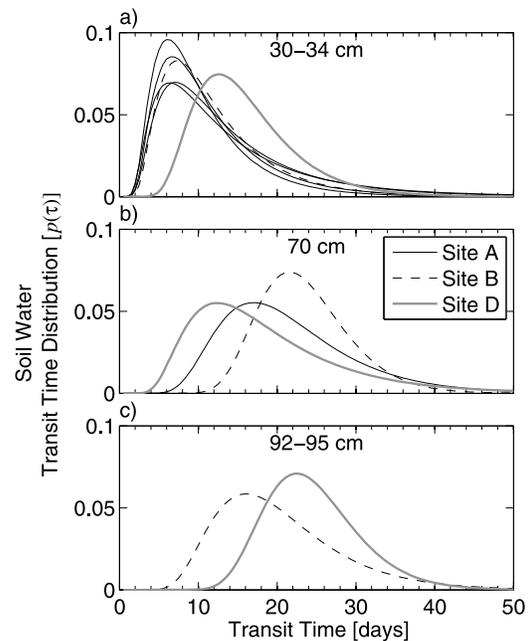
Figure 10. Soil water transit time distributions for sites A (lower slope), B (middle slope), and D (upper slope) for three different soil depths (a) 30–34, (b) 70, and (c) 92–95 cm. Additional details are given in Table 3.

flow [*Mosley*, 1979] or after peak streamflow [*Kendall et al.*, 1999], no study that we are aware of shows hillslope-streamflow hysteresis patterns that change direction over time.

[39] Our observations are consistent with the hydro-geomorphic model of *Sidle et al.* [2000], where during wet conditions, subsurface flow expands over greater slope distances, preferential flow commences (see discussion below), and moisture deficits are differentially exceeded in various hillslopes within the catchment [cf. *Jencso et al.*, 2009]. *Buttle et al.* [2004] and *Tromp-van Meerveld and McDonnell* [2006b] demonstrated recently that differential rates of filling of bedrock detention storage exert a nonlinear control on hillslope runoff contribution. Their work and our observed 30 mm threshold for hillslope subsurface flow initiation would suggest that the hysteresis loop reversal may be due to differential storage effects in other hillslopes that produce more rapid contributions compared to the gauged slope. We cannot confirm or refute the bedrock detention storage hypothesis; however, other processes such as bedrock exfiltration or enhanced connectivity of upslope regions that may lag in their contribution to the slope base (e.g., after networks are established [*Lehmann et al.*, 2007]) may also explain the observed hysteretic pattern between the hillslope and catchment runoff. Moreover, similar processes may explain the threshold response between precipitation and quick flow at the catchment outlet.

4.2. Nature and Extent of Hillslope-Stream Connections

[40] The nature and extent of hillslope and stream connectivity evolves through time as shallow processes become activated with increasing wetness and storm size. The importance of hillslope contributions to stream networks is often neglected during low-flow conditions when potential hillslope contributions are masked by the near-stream storage of groundwater. Our results indicate that hillslope contributions to the stream can be significant as shown by the large volumetric flow contribution of a single hillslope during the dry period (i.e., 15% of the total WS10 discharge). Localized seepage areas, such as this, would not be seen in most catchments due to the presence of near-stream storage zones, which were removed in WS10 by debris flows, exposing hillslope seepage areas. These seepage areas may be important for hyporheic processes [*Battin*, 1999; *Bencala*, 2000] and biogeochemical transformations that occur at the terrestrial-aquatic interface [*Cirmo and McDonnell*, 1997].

[41] After the catchment wet-up occurred, the hillslope contribution to the stream represented 2% of the total WS10 discharge, similar to the ratio of the hillslope drainage area to WS10 catchment area, and thus, a near 1:1 specific discharge relationship (see Figure 5). During wet periods, connectivity within the hillslope increased as the saturated zone expanded upward from the base of the slope at the soil-saprolite interface. At this interface, soil moisture remained near saturation (~85%) [*Ranken*, 1974] and consequently, was more easily converted to saturated conditions compared to shallower soil (30–70 cm), which might have been between 50 and 70% of saturation. Soil moisture responses at this depth were extremely rapid, as indicated by the 0.3 to 0.5 h response time of our 100 cm water content reflectometers.

[42] Studies on hillslopes with similarly high permeability and porosity soils that largely remain unsaturated, have suggested that rainfall intensities on relatively wet soils can produce pressure waves that cause rapid moisture response in the unsaturated zone [*Torres et al.*, 1998]. While soil moisture lag time estimates calculated from the centroid of rainfall inputs simplifies the convoluted pressure response to the rainfall intensity distribution, it does suggest rapid soil moisture changes occur at depth in the soil profile within the lower portion of the hillslope. The precise mechanism delivering water to this depth remains unclear. A pressure wave translation to depth augmenting soil moisture response cannot be rejected [see *Torres*, 2002]. On the other hand, the rapid Br^- breakthrough and the observed coincident soil moisture response suggest advective preferential flow transport is most plausible. Opportunities for solute transport from remote regions of the catchment seem feasible and increase over the time course of an event as transient saturated areas connect.

[43] Subsurface flow pore water velocities determined from our tracer experiment were similar to values observed by *Tsuboyama et al.* [1994] and *Sidle et al.* [1995] (0.508 m h^{-1}) for plot-scale Cl^- additions over a range of antecedent wetness conditions and application rates. *Anderson et al.* [1997] observed rather high velocities (3.6 m h^{-1}) of Br^- that was transported through saturated subsoils and bedrock. However, they did not observe any preferential flow through unsaturated soils and suggested a plug flow mechanism for soil water transport. *Harr* [1977] estimated that saturated zone Darcy fluxes directed entirely downslope could be between 0.1 and 0.25 m h^{-1} if midslope to upslope saturated areas along the subsoil contact were continuous and connected. Assuming θ is about 0.55 for saturated soils, pore water velocities would approximate velocities determined by our tracer breakthrough curves. This suggests that either contiguous saturated conditions existed between the tracer application and the trench and/or that preferential flow within predominantly unsaturated soils delivered tracer to the trench.

[44] Nevertheless, new water contributions from the hillslope and rapid tracer breakthrough observed at the slope base from the applied tracer experiment demonstrate that these hillslopes become hydrologically connected and contribute runoff from significant distances upslope. This is particularly striking since our experimental hillslope is unambiguously planar.

4.3. Transit Time as a Dynamic Connectivity Concept

[45] The runoff response from WS10 is extremely rapid and appears to be among the highest quick flow ratios reported in the literature [*Hewlett and Hibbert*, 1967; *Harr*, 1977; *McGlynn et al.*, 2002]. Yet, stormflow is dominated by preevent water with an average transit time exceeding 1 year (assuming that base flow was the a major contributor to preevent water). These observations are at the core of *Kirchner*'s [2003] old water paradox, where catchments promptly respond to rainfall events, but yield old water. Our results suggest that there are multiple sources of this "old" water, each with their own respective age distribution. For example, soil water transit times in the unsaturated zone were much younger (10–25 days) than base flow transit time (>1 year), but older than sources activated during storms,
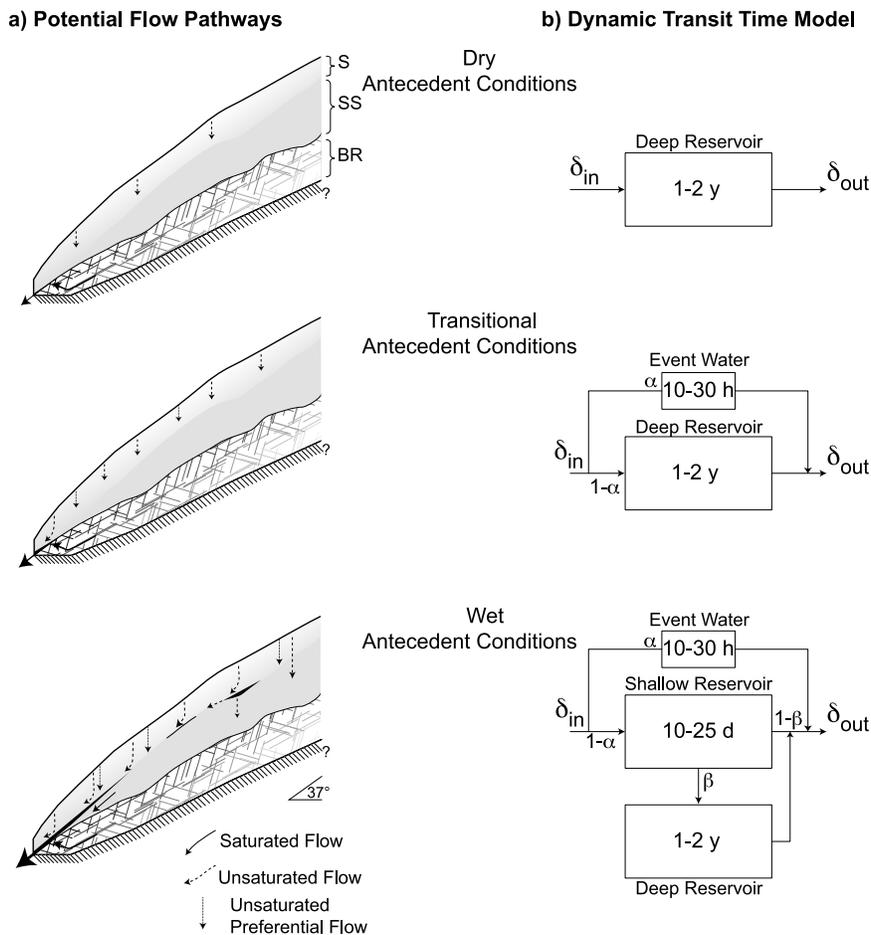
Figure 11. A diagram of a conceptual model illustrating (a) the variable flow pathways and (b) transit times contributing to runoff through three wetness phases. The hillslope is represented by a soil layer (S), a subsoil layer (SS) (weathered bedrock), and bedrock (BR) and shows hypothesized flow pathways during three different antecedent wetness stages (dry, transitional, and wet). Residence time components change under different wetness conditions and are illustrated by the conceptual reservoirs denoted with mean transit times; δ_{in} and δ_{out} designate tracer input and output signals, and the parameters α and β indicate the proportions of event water and deep subsurface water, respectively. Note that the illustrations are not drawn to scale.

which were reflected by the breakthrough of applied tracers and mean event water transit times (<30 h). We have developed a new conceptual model that illustrates how changes in hydrologic connectivity correspond to changes in the dominant source of water and hence dynamically control the water transit time discharging to the stream (Figure 11).

[46] The soil water TTDs show no evidence of downslope aging (consistent with *Asano et al.* [2002] and contrary to *Stewart and McDonnell* [1991]) and indicate a gradual vertical movement of water through upper soils between storms, which effectively "prime" the system with preevent water that is relatively young compared to bedrock seepage (Figures 11a, middle and 11b, middle). Soil water can then contribute to runoff through vertical and lateral preferential flow, as evidenced by the Br⁻ tracer experiment, and through the expanding saturated zone development during storms that tends to occur at major hydraulic conductivity contrasts (e.g., saprolite interface) (Figures 11a, middle and 11b, bottom). The latter soil water contribution process will

likely cause mixing with stored soil water and subsequently change the composition of lateral flow emulating older water [cf. *McDonnell*, 1990]. This effect would lessen over time as soil pore volumes are flushed multiple times yielding a more constant younger water source. Transit time estimates by *McGuire et al.* [2007] based on a simulation model that included dynamic interaction between the unsaturated and saturated zones representing largely interflow during events were between 54 and 69 days for the entire hillslope. These estimates are much younger than the isotope based estimates for base flow and suggest that soil water is a more dominant contribution to runoff that might be expected to increase as catchment wetness increases. This suggests that the shallow reservoir in Figures 11a (bottom) and 11b (bottom) is the primary control on transit time during wet periods or events.

[47] Estimated event water transit time distributions indicated a rapid response from preferential flow processes compared to the transit time distributions during drier con-

ditions, which were delayed due to transport through unsaturated soils (Figure 7). This suggests that the transit time of event water contributions likely vary over time even though evidence from only a few storms was presented in this study. The breakthrough of applied tracer also indicates that event water contributes from considerable upslope distances, which provides hillslope runoff to streamflow at the time scale of a storm event.

[48] While, the integration of transit time distributions from each of these sources would likely reveal a similar distribution as introduced by *Kirchner et al.* [2001], where runoff contains short-term responsive behavior and simultaneous long-term persistence or memory to past inputs, it is unclear how each of these sources with their respective transit time distributions are aggregated to produce the characteristic hillslope- or catchment-scale transit time distributions (i.e., how the values for parameters α and β in Figures 11a (bottom) and 11b (bottom) vary).

5. Concluding Remarks

[49] We examined the temporal dynamics of hillslope and catchment runoff responses using combined hydrometric, isotopic, and applied tracer approaches. We found that the hillslope runoff is nonlinearly related to the catchment runoff, hillslopes are capable of transporting solutes (tracer) to the stream from upslope areas over the time scale of a storm event, event water contributions are smaller for the hillslope than the catchment, and hillslope transit times can be longer than the catchment average. The nonlinear evolving relationship between hillslope runoff and streamflow through a wet-up period was controlled by moisture thresholds and expansion of saturated areas upslope. Saturated area expansion within a thin zone above weathered bedrock was inferred through soil moisture patterns, applied tracer breakthrough, large quick flow ratios, and previous studies at this site. Event water transit time distributions and rapid breakthrough from an applied upslope tracer addition, demonstrated that contributing areas extend far upslope during events. Despite these rapid transport processes and some contribution of event water from upslope regions, we found soil water and runoff mean transit times that were greater that the time scale of storm events. Soil water mean transit times exhibited no evidence of downslope aging and were between 10 and 25 days for shallow and deep soil, respectively. On the other hand, transit times of runoff from the hillslope and the catchment during nonstorm conditions were similarly between 1 and 2 years old. Our new dynamic conceptual model is based on variable physical flow pathways and transit times through changing antecedent wetness conditions—suggesting the importance of considering length and time scales in hydrologic connectivity studies.

References

Ali, G. A., and A. G. Roy (2009), Revisiting hydrologic sampling strategies for an accurate assessment of hydrologic connectivity in humid temperate systems, *Geogr. Compass*, 3(1), 350–374, doi:10.1111/j.1749-8198.2008.00180.x.

Anderson, S. P., W. E. Dietrich, D. R. Montgomery, R. Torres, M. E. Conrad, and K. Loague (1997), Subsurface flow paths in a steep, unchanneled catchment, *Water Resour. Res.*, 33(12), 2637–2653, doi:10.1029/97WR02595.

Asano, Y., T. Uchida, and N. Ohte (2002), Residence times and flow paths of water in steep unchannelled catchments, Tanakami, Japan, *J. Hydrol.*, 261(1–4), 173–192, doi:10.1016/S0022-1694(02)00005-7.

Battin, T. J. (1999), Hydrologic flow paths control dissolved organic carbon fluxes and metabolism in an alpine stream hyporheic zone, *Water Resour. Res.*, 35(10), 3159–3169, doi:10.1029/1999WR900144.

Bencala, K. E. (2000), Hyporheic zone hydrological processes, *Hydrol. Processes*, 14(15), 2797–2798, doi:10.1002/1099-1085(20001030)14:15<2797::AID-HYP402>3.0.CO;2-6.

Bonell, M. (1998), Selected challenges in runoff generation research in forests from the hillslope to headwater drainage basin scale, *J. Am. Water Resour. Assoc.*, 34(4), 765–785, doi:10.1111/j.1752-1688.1998.tb01514.x.

Bracken, L. J., and J. Croke (2007), The concept of hydrological connectivity and its contribution to understanding runoff-dominated geomorphic systems, *Hydrol. Processes*, 21(13), 1749–1763, doi:10.1002/hyp.6313.

Burns, D. A. (2002), Stormflow-hydrograph separation based on isotopes: The thrill is gone—What's next? *Hydrol. Processes*, 16(7), 1515–1517, doi:10.1002/hyp.5008.

Burt, T. P., and G. Pinay (2005), Linking hydrology and biogeochemistry in complex landscapes, *Prog. Phys. Geogr.*, 29, 297–316, doi:10.1191/0309133305pp450ra.

Buttle, J. M. (1994), Isotope hydrograph separations and rapid delivery of pre-event water from drainage basins, *Prog. Phys. Geogr.*, 18, 16–41, doi:10.1177/030913339401800102.

Buttle, J. M., P. J. Dillon, and G. R. Eerkes (2004), Hydrologic coupling of slopes, riparian zones and streams: An example from the Canadian Shield, *J. Hydrol.*, 287(1–4), 161–177, doi:10.1016/j.jhydrol.2003.09.022.

Cirmo, C. P., and J. J. McDonnell (1997), Linking the hydrologic and biogeochemical controls of nitrogen transport in near-stream zones of temperate-forested catchments: A review, *J. Hydrol.*, 199(1–2), 88–120, doi:10.1016/S0022-1694(96)03286-6.

Czarnomski, N. M., G. W. Moore, T. G. Pypker, J. Licata, and B. J. Bond (2005), Precision and accuracy of three alternative instruments for measuring soil water content in two forest soils of the Pacific Northwest, *Can. J. For. Res.*, 35, 1867–1876, doi:10.1139/x05-121.

Detty, J. M., and K. J. McGuire (2010a), Topographic controls on groundwater dynamics: Implications for hydrologic connectivity between hillslopes and riparian zones in a till mantled catchment, *Hydrol. Processes*, 24(16), 2222–2236, doi:10.1002/hyp.7656.

Detty, J. M., and K. J. McGuire (2010b), Threshold changes in storm runoff generation at a till mantled headwater catchment, *Water Resour. Res.*, 46, W07525, doi:10.1029/2009WR008102.

Epstein, S., and T. Mayeda (1953), Variation of ^{18}O content of water from natural sources, *Geochim. Cosmochim. Acta*, 4, 213–224, doi:10.1016/0016-7037(53)90051-9.

Freer, J., J. McDonnell, K. J. Beven, D. Brammer, D. Burns, R. P. Hooper, and C. Kendall (1997), Topographic controls on subsurface storm flow at the hillslope scale for two hydrologically distinct small catchments, *Hydrol. Processes*, 11(9), 1347–1352, doi:10.1002/(SICI)1099-1085(199707)11:9<1347::AID-HYP592>3.0.CO;2-R.

Freer, J., J. J. McDonnell, K. J. Beven, N. E. Peters, D. A. Burns, R. P. Hooper, and B. Aulenbach (2002), The role of bedrock topography on subsurface storm flow, *Water Resour. Res.*, 38(12), 1269, doi:10.1029/2001WR000872.

Genereux, D. (1998), Quantifying uncertainty in tracer-based hydrograph separations, *Water Resour. Res.*, 34(4), 915–919, doi:10.1029/98WR00010.

Gholz, H. L., G. M. Hawk, A. Campbell, J. K. Cromack, and A. T. Brown (1984), Early vegetation recovery and element cycles on a clear-cut watershed in western Oregon, *Can. J. For. Res.*, 14, 400–409.

Greenland, D. (1994), The Pacific Northwest regional context of the climate of the H. J. Andrews experimental forest long-term ecological research site, *Northwest Sci.*, 69, 81–96.

Hammermeister, D. P., G. F. Kling, and J. A. Vomocil (1982), Perched water tables on hillsides in western Oregon: I. Some factors affecting

their development and longevity, *Soil Sci. Soc. Am. J.*, *46*, 811–818, doi:10.2136/sssaj1982.03615995004600040030x.

Harr, R. D. (1977), Water flux in soil and subsoil on a steep forested slope, *J. Hydrol.*, *33*(1–2), 37–58, doi:10.1016/0022-1694(77)90097-X.

Harr, R. D., and F. M. McCorison (1979), Initial effects of clearcut logging on size and timing of peak flows in a small watershed in western Oregon, *Water Resour. Res.*, *15*(1), 90–94, doi:10.1029/WR015i001p00090.

Harr, R. D., and D. W. Ranken (1972), Movement of water through forested soils in steep topography, *Coniferous For. Biome Internal Rep. 117*, 19 pp., Univ. of Wash., Seattle.

Hewlett, J. D., and A. R. Hibbert (1967), Factors affecting the response of small watersheds to precipitation in humid areas, in *International Symposium on Forest Hydrology*, edited by W. E. Sopper and H. W. Lull, pp. 275–291, Pergamon, New York.

Hooper, R. P., B. T. Aulenbach, D. A. Burns, J. J. McDonnell, J. E. Freer, C. Kendall, and K. J. Beven (1998), Riparian control of stream-water chemistry: Implications for hydrochemical basin models, *IAHS Publ.*, *248*, 451–458.

Hoover, J. R. (1985), Evaluation of flow pathways in a sloping soil cross section, *Trans. ASAE*, *28*(5), 1471–1475.

Hopp, L., and J. J. McDonnell (2009), Connectivity at the hillslope scale: Identifying interactions between storm size, bedrock permeability, slope angle and soil depth, *J. Hydrol.*, *376*(3–4), 378–391, doi:10.1016/j.jhydrol.2009.07.047.

Jackson, C. R. (1992), Hillslope infiltration and lateral downslope unsaturated flow, *Water Resour. Res.*, *28*(9), 2533–2539, doi:10.1029/92WR00664.

James, M. E. (1978), Rock weathering in the central western Cascades, M.S. thesis, 119 pp., Univ. of Oreg., Eugene.

Jencso, K. G., B. L. McGlynn, M. N. Gooseff, S. M. Wondzell, K. E. Bencala, and L. A. Marshall (2009), Hydrologic connectivity between landscapes and streams: Transferring reach- and plot-scale understanding to the catchment scale, *Water Resour. Res.*, *45*, W04428, doi:10.1029/2008WR007225.

Joerin, C., K. J. Beven, I. Iorgulescu, and A. Musy (2002), Uncertainty in hydrograph separations based on geochemical mixing models, *J. Hydrol.*, *255*(1–4), 90–106, doi:10.1016/S0022-1694(01)00509-1.

Johnson, M. S., M. Weiler, E. G. Couto, S. J. Riha, and J. Lehmann (2007), Storm pulses of dissolved CO_2 in a forested headwater Amazonian stream explored using hydrograph separation, *Water Resour. Res.*, *43*, W11201, doi:10.1029/2007WR006359.

Kendall, K. A., J. B. Shanley, and J. J. McDonnell (1999), A hydrometric and geochemical approach to test the transmissivity feedback hypothesis during snowmelt, *J. Hydrol.*, *219*(3–4), 188–205, doi:10.1016/S0022-1694(99)00059-1.

Kennedy, V. C., G. W. Zellweger, and R. J. Avanzino (1979), Variation in rain chemistry during storms at two sites in northern California, *Water Resour. Res.*, *15*(3), 687–702, doi:10.1029/WR015i003p00687.

Kim, H. J., R. C. Sidle, R. D. Moore, and R. Hudson (2004), Throughflow variability during snowmelt in a forested mountain catchment, coastal British Columbia, Canada, *Hydrol. Processes*, *18*(7), 1219–1236, doi:10.1002/hyp.1396.

Kirchner, J. W. (2003), A double paradox in catchment hydrology and geochemistry, *Hydrol. Processes*, *17*(4), 871–874, doi:10.1002/hyp.5108.

Kirchner, J. W. (2006), Getting the right answers for the right reasons: Linking measurements, analyses, and models to advance the science of hydrology, *Water Resour. Res.*, *42*, W03S04, doi:10.1029/2005WR004362.

Kirchner, J. W., X. Feng, and C. Neal (2001), Catchment-scale advection and dispersion as a mechanism for fractal scaling in stream tracer concentrations, *J. Hydrol.*, *254*(1–4), 82–101, doi:10.1016/S0022-1694(01)00487-5.

Kreft, A., and A. Zuber (1978), On the physical meaning if the dispersion equation and its solutions for different initial and boundary conditions, *Chem. Eng. Sci.*, *33*, 1471–1480, doi:10.1016/0009-2509(78)85196-3.

Laudon, H., H. F. Hemond, R. Krouse, and K. H. Bishop (2002), Oxygen 18 fractionation during snowmelt: Implications for spring flood hydrograph separation, *Water Resour. Res.*, *38*(11), 1258, doi:10.1029/2002WR001510.

Lehmann, P., C. Hinz, G. McGrath, H. J. T.-v. Meerveld, and J. J. McDonnell (2007), Rainfall threshold for hillslope outflow: An emergent property of flow pathway connectivity, *Hydrol. Earth Syst. Sci.*, *11*(2), 1047–1063, doi:10.5194/hess-11-1047-2007.

Lischeid, G. (2008), Combining hydrometric and hydrochemical data sets for investigating runoff generation processes: Tautologies, inconsisten-

cies and possible explanations, *Geogr. Compass*, *2*(1), 255–280, doi:10.1111/j.1749-8198.2007.00082.x.

Lyon, S. W., and P. A. Troch (2010), Development and application of a catchment similarity index for subsurface flow, *Water Resour. Res.*, *46*, W03511, doi:10.1029/2009WR008500.

Lyon, S. W., S. L. E. Desilets, and P. A. Troch (2008), Characterizing the response of a catchment to an extreme rainfall event using hydrometric and isotopic data, *Water Resour. Res.*, *44*, W06413, doi:10.1029/2007WR006259.

Lyon, S. W., S. L. E. Desilets, and P. A. Troch (2009), A tale of two isotopes: Differences in hydrograph separation for a runoff event when using δD versus $\delta^{18}O$, *Hydrol. Processes*, *23*(14), 2095–2101, doi:10.1002/hyp.7326.

McDonnell, J. J. (1990), A rationale for old water discharge through macropores in a steep, humid catchment, *Water Resour. Res.*, *26*(11), 2821–2832, doi:10.1029/WR026i011p02821.

McDonnell, J. J., M. Bonell, M. K. Stewart, and A. J. Pearce (1990), Deuterium variations in storm rainfall: Implications for stream hydrograph separation, *Water Resour. Res.*, *26*(3), 455–458, doi:10.1029/WR026i003p00455.

McGlynn, B. L., and J. J. McDonnell (2003), Quantifying the relative contributions of riparian and hillslope zones to catchment runoff, *Water Resour. Res.*, *39*(11), 1310, doi:10.1029/2003WR002091.

McGlynn, B. L., J. J. McDonnell, and D. D. Brammer (2002), A review of the evolving perceptual model of hillslope flowpaths at the Maimai catchments, *N. Z. J. Hydrol.*, *257*, 1–26, doi:10.1016/S0022-1694(01)00559-5.

McGlynn, B. L., J. J. McDonnell, J. Seibert, and C. Kendall (2004), Scale effects on headwater catchment runoff timing, flow sources, and groundwater-streamflow relations, *Water Resour. Res.*, *40*, W07504, doi:10.1029/2003WR002494.

McGuire, K. J., and J. J. McDonnell (2006), A review and evaluation of catchment transit time modeling, *J. Hydrol.*, *330*(3–4), 543–563, doi:10.1016/j.jhydrol.2006.04.020.

McGuire, K. J., J. J. McDonnell, M. Weiler, C. Kendall, J. M. Welker, B. L. McGlynn, and J. Seibert (2005), The role of topography on catchment-scale water residence time, *Water Resour. Res.*, *41*, W05002, doi:10.1029/2004WR003657.

McGuire, K. J., M. Weiler, and J. J. McDonnell (2007), Integrating tracer experiments with modeling to assess runoff processes and water transit time, *Adv. Water Resour.*, *30*(4), 824–837, doi:10.1016/j.advwatres.2006.07.004.

Mosley, M. P. (1979), Streamflow generation in a forested watershed, *Water Resour. Res.*, *15*(4) 795–806, doi:10.1029/WR015i004p00795.

Murray, C. D., and J. M. Buttle (2005), Infiltration and soil water mixing on forested and harvested slopes during spring snowmelt, Turkey Lakes watershed, central Ontario, *J. Hydrol.*, *306*(1–4), 1–20, doi:10.1016/j.jhydrol.2004.08.032.

Nash, J. E., and J. V. Sutcliffe (1970), River flow forecasting through conceptual models, I, A discussion of principles, *J. Hydrol.*, *10*(3), 282–290, doi:10.1016/0022-1694(70)90255-6.

Ocampo, C. J., M. Sivapalan, and C. Oldham (2006), Hydrological connectivity of upland-riparian zones in agricultural catchments: Implications for runoff generation and nitrate transport, *J. Hydrol.*, *331*(3–4), 643–658, doi:10.1016/j.jhydrol.2006.06.010.

Peters, D. L., J. M. Buttle, C. H. Taylor, and B. D. LaZerte (1995), Runoff production in a forested, shallow soil, Canadian Shield basin, *Water Resour. Res.*, *31*(5), 1291–1304, doi:10.1029/94WR03286.

Pionke, H. B., W. J. Gburek, and G. J. Folmar (1993), Quantifying storm-flow components in a Pennsylvania watershed when ^{18}O input and storm conditions vary, *J. Hydrol.*, *148*(1–4), 169–187, doi:10.1016/0022-1694(93)90258-B.

Ranken, D. W. (1974), Hydrologic properties of soil and subsoil on a steep, forested slope, M.S. thesis, 114 pp., Oreg. State Univ., Corvallis.

Renshaw, C. E., X. Feng, K. J. Sinclair, and R. H. Dums (2003), The use of stream flow routing for direct channel precipitation with isotopically based hydrograph separations: The role of new water in stormflow generation, *J. Hydrol.*, *273*(1–4), 205–216, doi:10.1016/S0022-1694(02)00392-X.

Robson, A., K. Beven, and C. Neal (1992), Towards identifying sources of subsurface flow: A comparison of components identified by a physically based runoff model and those determined by chemical mixing techniques, *Hydrol. Processes*, *6*(2), 199–214, doi:10.1002/hyp.3360060208.

Sidle, R. C., Y. Tsuboyama, S. Noguchi, I. Hosoda, M. Fujieda, and T. Shimizu (1995), Seasonal hydrologic response at various spatial scales in a small forested catchment, Hitachi Ohta, Japan, *J. Hydrol.*, *168*(1–4), 227–250, doi:10.1016/0022-1694(94)02639-S.

Sidle, R. C., Y. Tsuboyama, S. Noguchi, I. Hosoda, M. Fujieda, and T. Shimizu (2000), Stormflow generation in steep forested headwaters: A linked hydrogeomorphic paradigm, *Hydrol. Processes*, *14*(3), 369–385, doi:10.1002/(SICI)1099-1085(20000228)14:3<369::AID-HYP943>3.0.CO;2-P.

Sklash, M. G. (1990), Environmental isotope studies of storm and snowmelt runoff generation, in *Processes in Hillslope Hydrology*, edited by M. G. Anderson and T. P. Burt, pp. 401–435, John Wiley, Chichester, U. K.

Smart, P. L., and I. M. S. Laidlaw (1977), An evaluation of some fluorescent dyes for water tracing, *Water Resour. Res.*, *13*(1), 15–33, doi:10.1029/WR013i001p00015.

Sollins, P., and F. M. McCorison (1981), Nitrogen and carbon solution chemistry of an old growth coniferous forest watershed before and after cutting, *Water Resour. Res.*, *17*(5), 1409–1418, doi:10.1029/WR017i005p01409.

Sollins, P., C. C. Grier, F. M. McCorison, K. J. Cromack, R. Fogel, and R. L. Fredriksen (1980), The internal element cycles of an old-growth Douglas-fir ecosystem in western Oregon, *Ecol. Monogr.*, *50*, 261–285, doi:10.2307/2937252.

Sollins, P., K. J. Cromack, F. M. McCorison, R. H. Waring, and R. D. Harr (1981), Changes in nitrogen cycling at an old-growth Douglas-fir site after disturbance, *J. Environ. Qual.*, *10*, 37–42, doi:10.2134/jeq1981.00472425001000010007x.

Spence, C., and M. K. Woo (2003), Hydrology of subarctic Canadian Shield: Soil-filled valleys, *J. Hydrol.*, *279*(1–4), 151–166, doi:10.1016/S0022-1694(03)00175-6.

Stewart, M. K., and J. J. McDonnell (1991), Modeling base flow soil water residence times from deuterium concentrations, *Water Resour. Res.*, *27*(10), 2681–2693, doi:10.1029/91WR01569.

Stieglitz, M., J. Shaman, J. McNamara, V. Engel, J. Shanley, and G. W. Kling (2003), An approach to understanding hydrologic connectivity on the hillslope and the implications for nutrient transport, *Global Biogeochem. Cycles*, *17*(4), 1105, doi:10.1029/2003GB002041.

Swanson, F. J., and M. E. James (1975), Geology and geomorphology of the H. J. Andrews Experimental Forest, western Cascades, Oregon, *Res. Pap. PNW-188*, 14 pp., Pac. Northwest For. and Range Exp. Stn., Portland, Oreg.

Tani, M. (1997), Runoff generation processes estimated from hydrological observations on a steep forested hillslope with a thin soil layer, *J. Hydrol.*, *200*(1–4), 84–109, doi:10.1016/S0022-1694(97)00018-8.

Torres, R. (2002), A threshold condition for soil-water transport, *Hydrol. Processes*, *16*(13), 2703–2706, doi:10.1002/hyp.5060.

Torres, R., W. E. Dietrich, D. R. Montgomery, S. P. Anderson, and K. Loague (1998), Unsaturated zone processes and the hydrologic response of a steep, unchanneled catchment, *Water Resour. Res.*, *34*(8), 1865–1879, doi:10.1029/98WR01140.

Triska, F. J., J. R. Sedell, K. Cromack, S. V. Gregory, and F. M. McCorison (1984), Nitrogen budget for a small coniferous forest stream, *Ecol. Monogr.*, *54*, 119–140, doi:10.2307/1942458.

Tromp-van Meerveld, H. J., and J. J. McDonnell (2006a), Threshold relations in subsurface stormflow: 1. A 147 storm analysis of the Panola hillslope, *Water Resour. Res.*, *42*, W02410, doi:10.1029/2004WR003778.

Tromp-van Meerveld, H. J., and J. J. McDonnell (2006b), Threshold relations in subsurface stormflow: 2. The fill and spill hypothesis, *Water Resour. Res.*, *42*, W02411, doi:10.1029/2004WR003800.

Tsuboyama, Y., R. C. Sidle, S. Noguchi, and I. Hosoda (1994), Flow and solute transport through the soil matrix and macropores of a hillslope segment, *Water Resour. Res.*, *30*(4), 879–890, doi:10.1029/93WR03245.

Turton, D. J., C. T. Haan, and E. L. Miller (1992), Subsurface flow responses of a small forested catchment in the Ouachita Mountains, *Hydrol. Processes*, *6*, 111–125, doi:10.1002/hyp.3360060110.

van Verseveld, W. J. (2007), Hydro-biogeochemical coupling at the hillslope and catchment scale, Ph.D. thesis, 216 pp., Oreg. State Univ., Corvallis.

van Verseveld, W. J., J. J. McDonnell, and K. Lajtha (2009), The role of hillslope hydrology in controlling nutrient loss, *J. Hydrol.*, *367*(3–4), 177–187, doi:10.1016/j.jhydrol.2008.11.002.

Vidon, P. G. F., and A. R. Hill (2004), Landscape controls on the hydrology of stream riparian zones, *J. Hydrol.*, *292*(1–4), 210–228, doi:10.1016/j.jhydrol.2004.01.005.

Weiler, M., B. L. McGlynn, K. J. McGuire, and J. J. McDonnell (2003), How does rainfall become runoff? A combined tracer and runoff transfer function approach, *Water Resour. Res.*, *39*(11), 1315, doi:10.1029/2003WR002331.

Weyman, D. R. (1970), Throughflow on hillslopes and its relation to the stream hydrograph, *Bull. Int. Assoc. Sci. Hydrol.*, *15*(3), 25–33, doi:10.1080/02626667009493969.

Weyman, D. R. (1973), Measurements of the downslope flow of water in a soil, *J. Hydrol.*, *20*(3), 267–288, doi:10.1016/0022-1694(73)90065-6.

Whipkey, R. Z. (1965), Subsurface storm flow from forested slopes, *Bull. Int. Assoc. Sci. Hydrol.*, *10*(2), 74–85, doi:10.1080/02626666509493392.

Wilson, G. V., P. M. Jardine, R. J. Luxmoore, L. W. Zelazny, D. A. Lietzke, and D. E. Todd (1991), Hydrogeochemical processes controlling subsurface transport from an upper subcatchment of Walker Branch watershed during storm events. 1. Hydrologic transport processes, *J. Hydrol. (3–4)*, *123*, 297–316, doi:10.1016/0022-1694(91)90096-Z.

Woods, R., and L. Rowe (1996), The changing spatial variability of subsurface flow across a hillside, *N. Z. J. Hydrol.*, *35*(1), 51–86.

J. J. McDonnell, Department of Forest Engineering, Resources and Management, Oregon State University, Corvallis, OR 97331, USA. (jeff.mcdonnell@oregonstate.edu)

K. J. McGuire, Virginia Water Resources Research Center, Virginia Polytechnic Institute and State University, Blacksburg, VA 24061, USA. (kevin.mcguire@vt.edu)